Springer

KSME

Journal of Mechanical Science and Technology 33 (7) (2019) 3187~3192
www.springerlink.com/content/1738-494x(Print)/1976-3824(Online)
DOI 10.1007/s12206-019-0613-6

Acoustic noise measurement in counter-rotating propellers †

Pin Liu[1,*], Fumiha Odo[2], Tengen Murakami[1] and Toshiaki Kanemoto[1]

[1]*Institute of Ocean Energy, Saga University, Saga, Japan*
[2]*Grad of Kyushu Institute of Technology, Kitakyushu, Japan*

(Manuscript Received February 7, 2019; Revised March 28, 2019; Accepted April 18, 2019)

Abstract

The acoustic noise and flow condition of tandem propellers in a horizontal axis-type tidal stream power unit, which is composed of counter-rotating propellers and double-rotational armature-type generator without traditional stators, were experimentally investigated. The front and rear propellers rotate in opposite directions and drive the inner and outer armatures, respectively; the rotational torque of the front propeller coincides with the torque of the rear propeller. The front blade profile exerts a great effect on noise generation from the tandem propellers, but the effect of the rear blade profile is comparatively small. The sound pressure level is largely concentrated at low frequencies, and most predominant frequencies can be predicted by Hanson's method. These predominant frequencies are mainly caused by the tip vortex shedding from the front and rear blades in the counter-rotating propellers. The vortex shedding from the front blade does not affect the rear blade. As a result, the acoustic noise is weakened as long as the diameter of the rear propeller is smaller than the diameter of the front propeller.

Keywords: Acoustic noise; Blade profile; Counter-rotating; Tandem propellers; Tip vortex

1. Introduction

With the rapid increase in fuel consumption, stream energy has attracted attention because it can serve as a renewable and clean energy resource. Horizontal axis-type turbines have been widely applied not only to wind energy resources but also to tidal stream energy resources from oceans [1]. A horizontal-axis counter rotating-type power unit, in which the tandem propellers, including front and rear propellers, drive rotational inner and outer armatures in generators, has also been developed [2]. This type of power unit is used to convert wind and tidal energy [3, 4], and its efficiency has been improved [5-7].

The acoustic noise caused by counter-rotating propellers has also been studied, and results indicate that the main noise source is due to the flow interaction between tandem propellers and that the dominant power spectral density (PSD) is at the frequency of the blade passing interaction between tandem propellers [8]. The diameter of the front rotor is designed to be reasonably larger than the rear diameter with consideration of the tip vortex shedding from the front propeller without affecting the rear propeller [9]. The mechanism of noise formation in counter-rotating propellers should be investigated, and noise prediction needs to be considered in the blade design process. In the present study, the acoustic noise and flow condition in tandem propellers composed of different front and rear blade profiles are investigated experimentally in a wind tunnel.

*Corresponding author. Tel.: +81 952288624, Fax.: +81 952288595
E-mail address: liu.pin379@mail.kyutech.jp
† Recommended by Associate Editor Doo Ho Lee

2. Acoustic noise and flow condition measurement in tandem propellers

2.1 Preparation of model blades

The blade profiles of the counter-rotating propellers are shown in Fig. 1, in which all blade elements are formed with MEL002 airfoil [10]. Front blade G and rear blades G and K are formed with cambered airfoils and twisted in pitch direction to achieve the desirable angle of attack (7 degrees in front blade G, 11 degrees in rear blade G with front blade G or H, 10 degrees in rear blade K with front blade H) and satisfy the free vortex-type swirling flow at the ideal flow condition without distortion. Front blade H is formed with a symmetrical airfoil element close to the hub to discharge a swirl-less flow; thus, the rear propeller can get wind energy from the front propeller. The blade chord length decreases from the hub to the tip in the radial direction, except for rear blade K with a constant length. In the following discussion, tandem propellers are labeled as follows: For instance, tandem HG, which is composed of front blade H and rear blade G. The radius of the front propeller is R_F = 115 mm, and the ratio of the rear propeller to the front propeller is R_R/R_F = 0.84. The numbers of

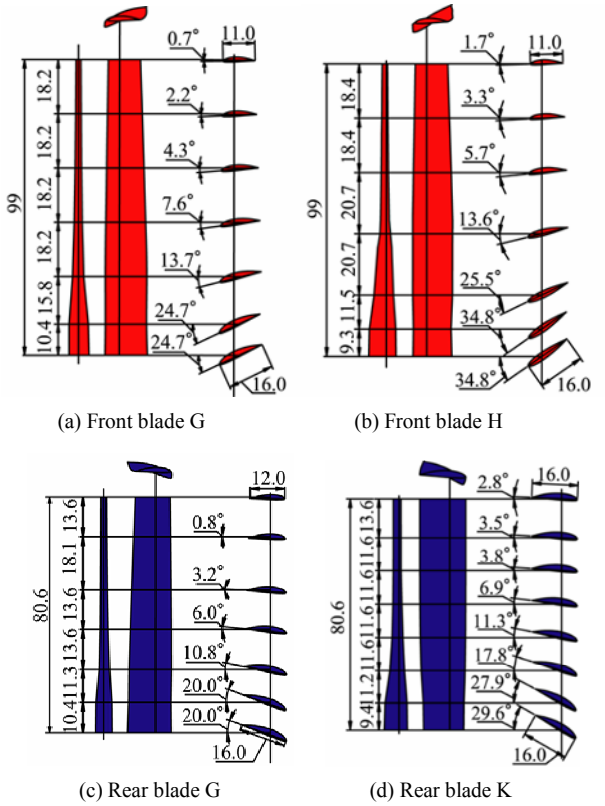

(a) Front blade G (b) Front blade H

(c) Rear blade G (d) Rear blade K

Fig. 1. Blades.

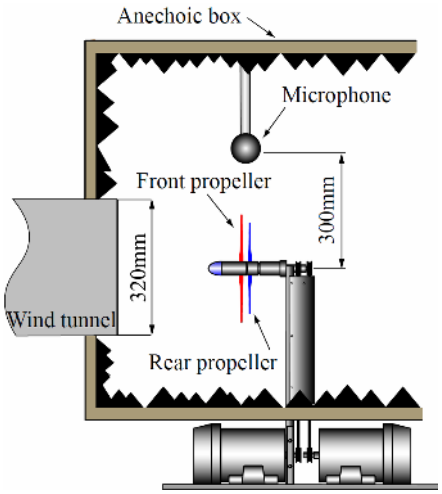

Fig. 2. Anechoic box for experiment.

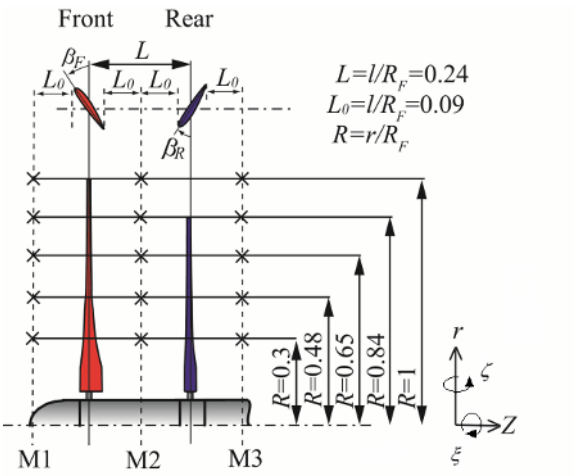

Fig. 3. Model propellers and measurement points.

blades in the front and rear propellers are Z_F = 3 and Z_R = 5, respectively. These values were optimized in the previous research [11]. The dimensionless axial distance between the front and rear propellers is set to $L = l/R_F = 0.16$ in the acoustic noise investigation and to 0.24 for the flow investigation to cordon the space of hot-wire probes.

2.2 Measurements of acoustic noise and flow

The acoustic noise and flow are measured in an anechoic box setting at the nozzle outlet of a wind tunnel, as shown in Fig. 2. The anechoic box is a 1 m x 1 m x 1 m cube with a waved internal surface comprising small pieces of foamed plastic that crumbles arbitrarily. The high-functioning sound level meter Onosokki LA-5560 and wideband microphone Onosokki MI-1233 with a titanium vibration film are used; both devices can maintain a high stability. The frequency range is from 20 Hz to 20 kHz, and the sensitivity of the wideband microphone is −29 dB ± 3 dB re. 1 V/Pa. Measurement technologies were presented in previous studies [8, 9] and are described herein to facilitate the following discussions. The model propellers are set at 300 mm downstream from the nozzle outlet, and all investigations are conducted at a stream velocity of V_{in} = 9 m/s. The driving system with a quiet axial fan of the wind tunnel is located outside the experimental room to eliminate background noise as much as possible. The microphone is placed 300 mm away from the model propellers in the vertical direction relative to the stream. The rotational speeds are adjusted with an inverter system, the shaft of which is connected to an isolated motor through a pulley system with timing belts.

The flow around the propellers is investigated at the position marked with "X" in Fig. 3 by a hot-wire anemometer with X-type probes (upstream type MODEL 0249R-T5 and cross type MODEL 0250R-T5 of KANOMAX), where the radius R and distances L and L_0 are divided by the radius of the front propeller R_F. The probes have two crossed hot wires in 90 degrees and can measure not only the velocity but also the flow direction in the two-dimensional plane. The vorticities ζ in the radial direction and ξ in the axial/stream direction are estimated from Eqs. (1) and (2) in the right-handed system of r, θ and z.

$$\zeta = \partial V_\theta / \partial Z - \partial V_Z / r\partial\theta \cong -\partial V_Z / r\partial\theta \quad (1)$$

$$\xi = \partial V_r / r\partial\theta - \partial(rV_\theta) / r\partial r \cong \partial V_r / r\partial\theta \quad (2)$$

where V_r, V_θ and V_z are the velocity components in the radial, tangential, and axial directions, respectively. The second equa-

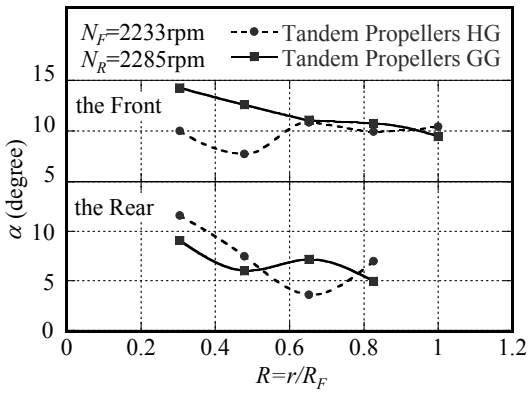

Fig. 4. Angle of attack distributions of tandem propellers GG and HG at V_{in} = 9 m/s.

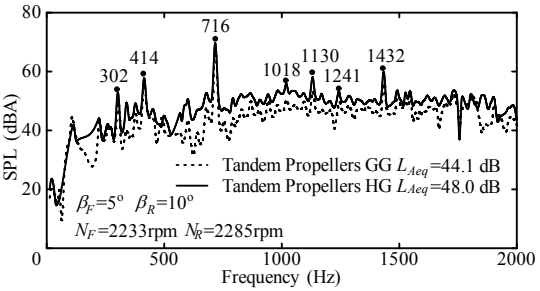

Fig. 5. Sound power spectrum distributions of tandem propellers GG and HG at V_{in} = 9 m/s.

tion is simplified considering that the swirling velocity is almost constant in the axial direction z and has a free vortex distribution, except for Front Blade H close to the hub.

2.3 Effects of front blade profile on acoustic noise

The angle of attack of tandem propellers GG and HG is presented in Fig. 4, in which the front and rear rotational speeds are N_F = 2233 min^{-1} and N_R = 2285 min^{-1}, respectively; and the front and rear blade setting angles (Fig. 3) measured from the tangential direction are β_F = 5 degrees and β_R = 10 degrees at the blade tips, respectively. The Reynolds number estimated from the relative velocity and the chord at the front blade tip is Re = 4.1 x10^4 for front blades G and H, which means that the flow is laminar flow but will not affect the analysis of the sound pressure distribution of the tandem propellers, although the flow is turbulence flow in real cases. As for the tandem propeller HG, in comparison with tandem propeller GG, the angle of attack α is larger for the front blade and smaller for the rear blade close to the hub wall as expected (see Fig. 1).

The power spectrum distributions measured by A-weighted sound pressure level *SPL* of tandem propellers GG and HG are shown in Fig. 5. The A-weighted overall sound pressure levels (OASPLs) of tandem propeller GG and HG are 71.4 and 75.2 dB, respectively. The sound pressure level of tandem propeller HG is higher than that of tandem propeller GG

Table 1. Dominant frequencies of tandem propellers GG and HG.

Sound harmonic	Load harmonic	Frequency
m	k	f Hz
1	1	302
	2	414
2	3	716
3	4	1018
	5	1130
	6	1241
4	6	1432

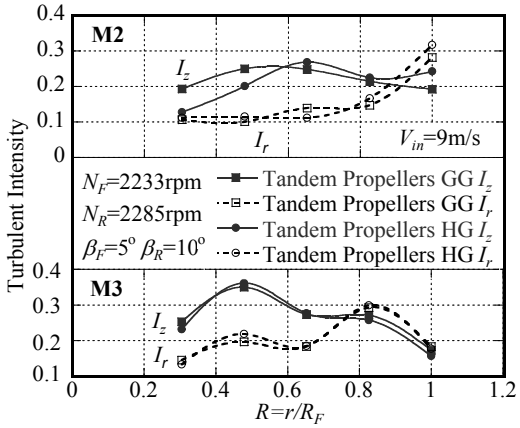

Fig. 6. Turbulence intensity distributions of tandem propellers GG and HG.

throughout the frequency possibly because of the flow separation close to the hub. The equivalent continuous A-weighted sound pressure level L_{Aeq} from tandem propeller HG is approximately 4 dB higher than that from tandem propeller GG, as evaluated by averaging the energy of sound pressure level in the measured time. The peaks of the sound power spectrum are at almost the same frequencies, and these dominant frequencies can be predicted by Hanson's method shown in Table 1 [12]; Hanson proposed to predict the predominant frequency by $f = |mZ_RN_R+kZ_FN_F|$ caused by the flow interaction in counter-rotating propellers; here, m and k are natural number and integral number coefficients, respectively, for the harmonics of blade passing frequencies (BPFs) Z_RN_R at the rear propeller and Z_FN_F at the front propeller.

The turbulence intensities in the axial and radial directions, I_z and I_r, defined by Eqs. (3) and (4) are presented in Fig. 6.

$$I_z = \sqrt{\overline{v_z'^2}} / \bar{v} \tag{3}$$

$$I_r = \sqrt{\overline{v_r'^2}} / \bar{v} \,. \tag{4}$$

At section M3 downstream of the rear propeller, the turbulent intensities in the axial and radial directions have almost the same values because the rear blade profiles are the same, whereas I_z is larger than I_r at a small radius. At section M2

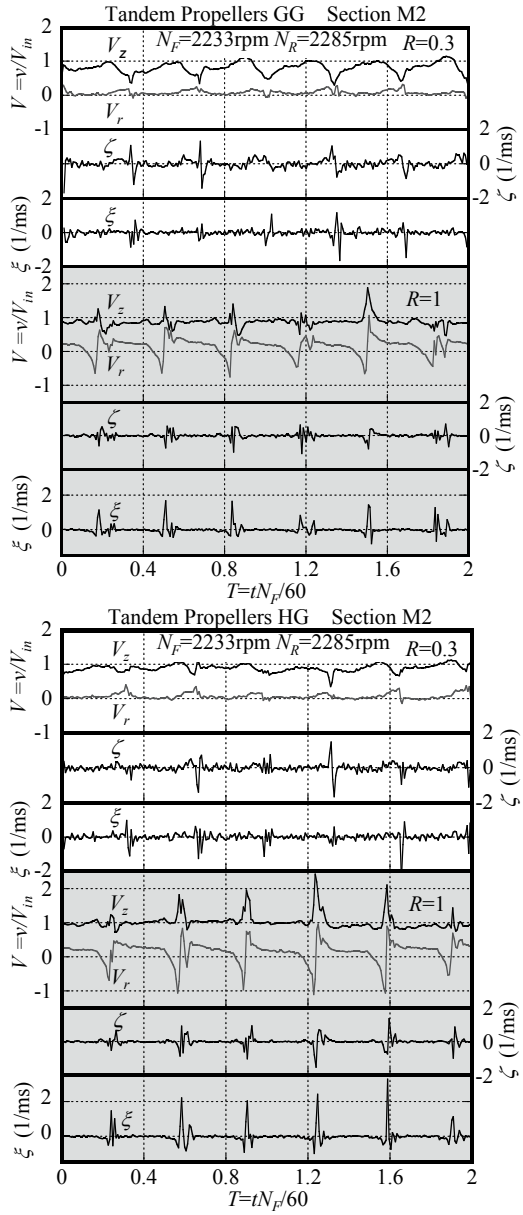

Fig. 7. Velocity fluctuation and vorticity components of tandem propellers GG and HG at section M2.

downstream of the front impeller, the turbulence intensity in the axial directions is affected by the front blade profile but is scarcely affected by the rear blade profile, which is far from section M2, that is, front blade G has a large-scale flow separation induced by the large angle of attack α. (see Fig. 4) that promotes turbulence intensity. The intensity in the radial direction I_r increases with an increase in the radius that possibly originates from the tip vortex [13].

The velocity and vorticity vary in response to passing time t, as shown in Fig. 7, where V_z and V_r are the axial and radial velocity components divided by the incoming flow velocity V_{in}, respectively; ξ and ζ are the axial and radial vorticity components, respectively; and time t corresponds to the flow distributions from the pressure surface to the suction surface

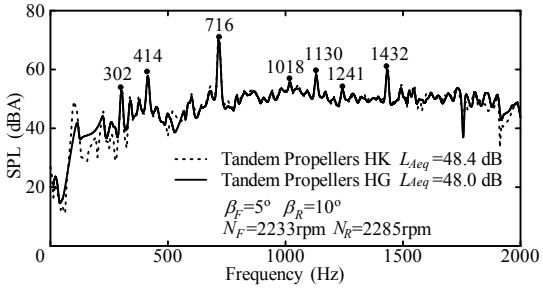

Fig. 8. Spectral distribution of tandem propellers HK and HG at V_{in} = 9 m/s.

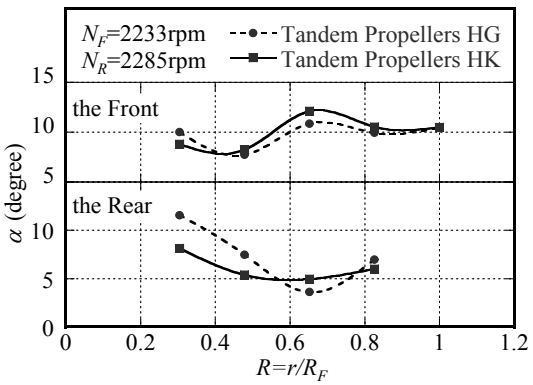

Fig. 9. Angle of attack of tandem propellers HG and HK at V_{in} = 9 m/s.

between adjacent blades. Wake flows are observed on blade tip R = 1 at section M2 downstream of the front propeller, and the radial velocity V_r and the vorticity in the radial direction ζ suddenly fluctuate from negative to positive values close to the trailing edge. The velocities V_z and V_r change obviously along with vorticity in the stream direction ξ at radius R = 1 corresponding to the blade tip of the tandem propeller HG. Vorticity ξ is mainly induced from the vortex shedding from the blade tip and rotates clockwise against the front blade rotation, in which velocity V_r takes an opposite distribution because of the flow measured at the static position while the blade is rotating. With a decrease in radius (R = 0.3), the effect of the blade profile on velocity and vorticity declines, but the wake flow from front blade G with a large angle of attack is confirmed. The low angle of attack near the hub of front blade H makes the turbulence intensity in the axial direction comparatively weak. Nevertheless, the turbulence intensity in the axial and radial components is enlarged near the blade tip, thereby increasing the noise (Fig. 6 at section M2) in comparison with that in front blade G. The shed vortex from the front blade tip associated with an increase in turbulence intensity adds to the acoustic noise.

2.4 Effects of rear blade profile on acoustic noise

Fig. 8 shows the power spectrum of the acoustic noise emitted from tandem propellers HG and HK, in which the rotational speeds and blade setting angles are the same as those

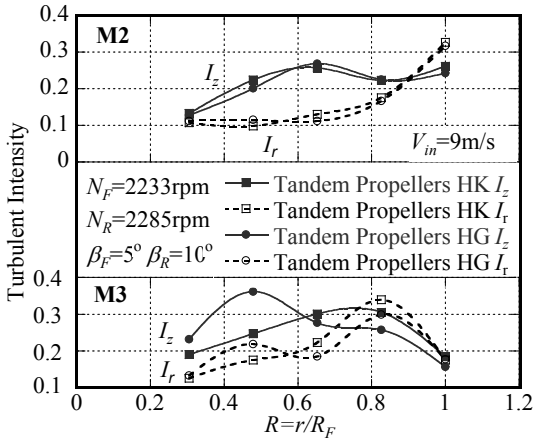

Fig. 10. Turbulence intensity distributions of tandem propellers HG and HK.

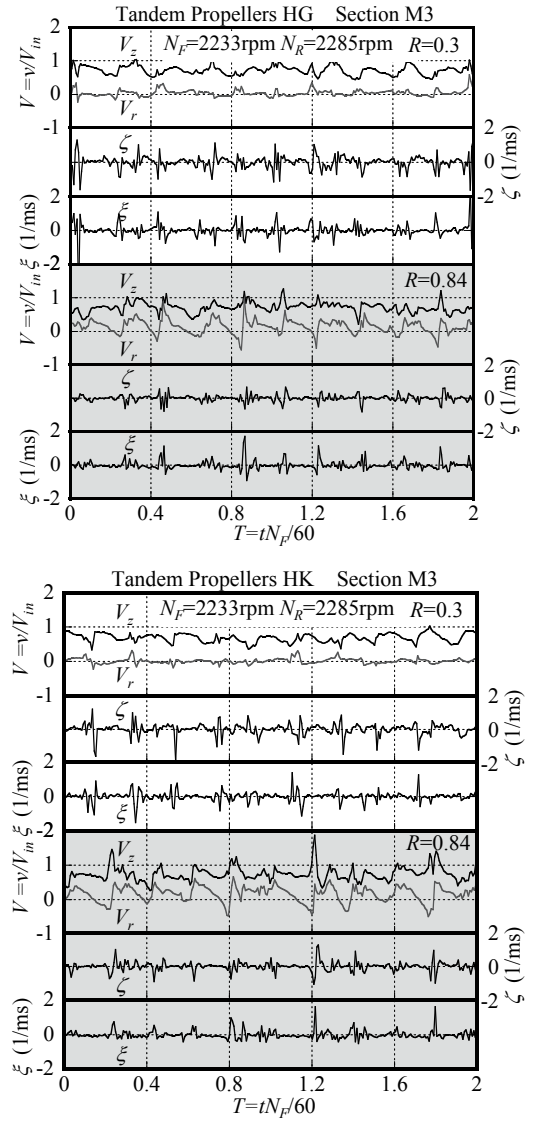

Fig. 11. Velocity fluctuation and vorticity components of tandem propellers HG and HK at section M3.

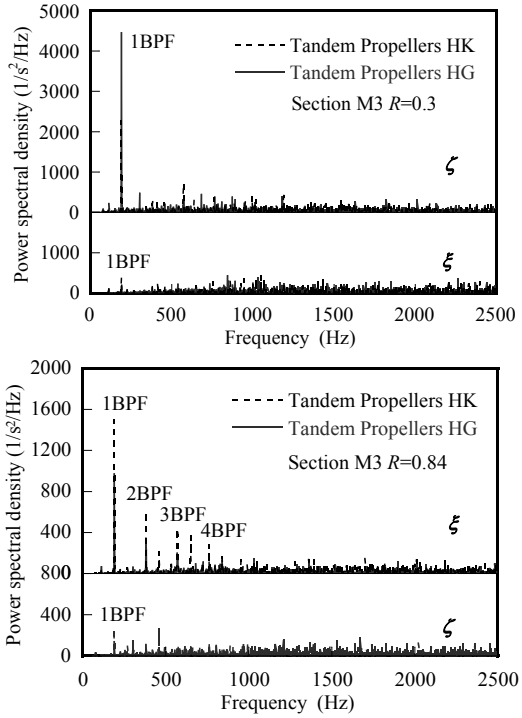

Fig. 12. PSD of vorticity at section M3.

discussed previously. The A-weighted OASPLs of tandem propellers HG and HK are 75.2 and 75.6 dB, respectively. In comparison with that in Fig. 5, the sound pressure level *SPL* and the equivalent continuous A-weighted sound pressure level L_{Aeq} in Fig. 8 are scarcely affected by the rear blade profile, and the dominant frequencies can be estimated with Hanson's method. Such results can be understood with the angle of attack shown in Fig. 9, where the angles of attack α are almost the same for both tandem propellers, although the twisted angle of rear blade K is slightly larger than that of rear blade G (see Fig. 1).

The turbulence intensities in the axial and radial directions, I_z, I_r, are presented in Fig. 10. The rear blade profile affects the intensity at section M3 downstream of the rear blade in contrast to the intensity depicted in Fig. 6. The intensities of tandem propeller HK are lower than the intensities of tandem propeller HG near the hub, and they have a slightly inverse tendency near the blade tip affected by the tip vortex. The chord length of rear blade G gradually decreases from hub to tip, possibly depressing the generation of tip vortex effectively [9].

Fig. 11 shows the velocity and vorticity fluctuations at section M3 downstream of the rear propeller. These values fluctuate naturally, and the fluctuations of the velocities are noticeably near the blade tip region (R = 0.84). The PSD of vorticity at section M3 is shown in Fig. 12. The distribution of vorticity power in the frequency domain is presented, and the unit is the unit of vorticity squared over the frequency (1/s^2/Hz). The PSD of vorticity dominates at the BPF of the rear propeller, the PSD of the vorticity in the radial direction

ζ is large at the hub side (R = 0.3) of tandem propeller HG, and the PSD of the vorticity in the stream direction ξ is large at the tip side (R = 0.84) of tandem propeller HK. These results may be caused by the difference in shear flow in the wake affected by the boundary layer and the vortex shedding from the blade tip affected by the blade load.

3. Conclusions

The acoustic noise and flow condition in tandem propellers were investigated in a wind tunnel. Three main results were obtained. First, the front blade affects the sound pressure level, and the dominant frequency can be predicted using Hanson's method; however, the effect of the rear blade is comparatively small. Second, predominant frequencies are mainly caused by the tip vortex shedding from the front and rear blades in counter-rotating propellers. Third, noise power density is largely concentrated at the BPF.

References

[1] P. L. Fraenkel, Power from marine currents, *Journal of Power and Energy*, 216 (1) (2002) 1-14.

[2] K. Kubo and T. Kanemoto, Development of intelligent wind turbine unit with tandem wind rotors and double rotational armatures (2nd Report, Characteristics of tandem wind rotors), *Journal of Fluid Science and Technology*, 3 (3) (2008) 370-378.

[3] Y. Usui, T. Kanemoto and K. Hiraki, Counter-rotating type tidal stream power unit boarded on pillar (Performances and flow conditions of tandem propellers), *Journal of Thermal Science*, 22 (6) (2013) 580-585.

[4] B. Huang, G. J. Zhu and T. Kanemoto, Design and performance enhancement of a bi-directional counter-rotating type horizontal axis tidal turbine, *Ocean Engineering*, 128 (2016) 116-123.

[5] B. Huang, Y. Usui, K. Takaki and T. Kanemoto, Optimization of blade setting angles of a counter-rotating type horizontal-axis tidal turbine using response surface methodology and experimental validation, *International Journal of Energy Research*, 40 (5) (2016) 610-617.

[6] B. Huang and T. Kanemoto, Performance and internal flow of a counter-rotating type tidal stream, *Journal of Thermal Science*, 24 (5) (2015) 410-416.

[7] B. Huang and T. Kanemoto, Multi-objective numerical optimization of the front blade pitch angle distribution in a counter-rotating type horizontal-axis tidal turbine, *Renewable Energy*, 81 (2015) 837-844.

[8] K. Kubo, N. Mihara, A. Enishi and T. Kanemoto, Acoustic noise from tandem wind rotors of intelligent wind power unit, *Journal of Thermal Science*, 19 (2) (2010) 120-125.

[9] F. Odo, A. M. Galal, A. Enishi and T. Kanemoto, Effect of angle of attack and blade tip vortex on the noise level of tandem wind rotors of an intelligent wind power unit, *Journal of Environmental Science and Engineering*, *A* 2 (12) (2013) 736-743.

[10] National Institute of Advanced Industrial Science and Technology, *http://riodb.ibase.aist.go.jp/db060* (2006).

[11] T. Kanemoto and A. M. Galal, Development of intelligent wind turbine generator with tandem wind rotors and double rotational armatures, *JSME International Journal*, B 49 (2) (2006) 450-457.

[12] D. B. Hanson, Noise of counter-rotation propellers, *Journal of Aircraft*, 22 (7) (1985) 609-617.

[13] P. Liu, X. S. Wei, M. W. Heo and T. Kanemoto, Vortices shedding from blade tips of counter-rotating propellers installed in tidal stream power unit, *Proc. of 6th Asian Joint Workshop on Thermophysics and Fluid Science*, GuiLin, China (2016) 1-5.

Pin Liu is currently a postdoctoral researcher at the Institute of Ocean Energy, Saga University, Japan. She received her doctoral degree in engineering in the field of science and advanced technology from Saga University in 2014. Her research interests include axial flow fans, tidal turbines, and relative research in CFD simulation, PIV, and noise analysis.